J. Fluid Mech. (1976), *vol.* 76, *part* 4, *pp.* 689–709
Printed in Great Britain

Some problems concerning the production of a linear shear flow using curved wire-gauze screens

By I. P. CASTRO

Central Electricity Generating Board, Marchwood Engineering Laboratories, Marchwood, Southampton, England

(Received 4 March 1975 and in revised form 21 May 1976)

The flow of an incompressible fluid through a curved wire-gauze screen of arbitrary shape is reconsidered. Some inconsistencies in previously published papers are indicated and the various approximations and linearizations (some of which are necessary for a complete analytic solution) are discussed and their inadequacies demonstrated. Attention is concentrated on the common practical problem of calculating the screen shape required to produce a linear shear flow and experimental work is presented which supports the contention that the theoretical solutions proposed by Elder (1959) – subsequently discussed by Turner (1969) and Livesey & Laws (1973) – and Lau & Baines (1968) are inadequate, although, for the case of small shear, Elder's theory appears to be satisfactory. Since, in addition, there are inevitable difficulties concerning both the value of the deflexion coefficient appropriate to any particular screen and inhomogeneities in the screen itself, it is concluded that the preparation of a curved screen to produce the commonly required moderate to large linear shear flow is bound to be somewhat empirical and should be attempted with caution.

1. Introduction

In recent years there has been a considerable upsurge of interest in what is rather loosely termed 'architectural' aerodynamics. Although there are now well-established methods of simulating a neutral atmospheric boundary layer, to gain a proper understanding of the bluff-body flows typical of real-life situations it is usually desirable, and indeed probably necessary, to investigate the effects of upstream turbulence and shear separately. It is evident that, whilst there is an increasing volume of data concerning the effects of upstream turbulence (of varying intensities and scales), there is much less information available for the case of an upstream turbulence-free shear flow. The desire to improve this situation led the author to investigate the various previously proposed methods of producing a linear shear flow in a wind tunnel.

One of the earliest suggestions was that of Owen & Zienkiewicz (1957); they showed that a planar resistance with a linear variation of drag across its surface produced a linear sheared velocity profile when placed normal to a uniform incident stream. A grid of rods of the required theoretical spacing was found experimentally to give a good linear profile of the correct shear. Cockrell & Lee

(1966) used a similar method to produce nonlinear shear flows. A disadvantage of this technique is the relatively high turbulence levels produced: typically 3–4 % even for rods of only 1 mm diameter. For the purposes described above it is desirable to keep turbulence levels as low as possible. Taylor & Batchelor (1949) showed that a gauze placed normal to the flow tends in general to reduce any departures from non-uniformity in the flow (which is, of course, why screens are used in wind-tunnel settling chambers as 'smoothing' screens). Elder (1959), who based much of his work on that of Davis (1957), was the first to calculate the shape of a curved gauze required to produce a linear shear profile and his work has stimulated some more recent workers to attempt to produce a linear shear flow which has an acceptably low turbulent intensity (typically 0·5 % or less). There are one or two errors in Elder's paper, which have been pointed out and discussed by Turner (1969), Lau & Baines (1968) (whose own theory differs in important respects from that of Elder) and, more recently, Livesey & Laws (1973). Unfortunately, a careful reading of these papers reveals further difficulties, some of which are serious, which make it very difficult to apply the results effectively.

Since the production of a linear shear flow is usually only an initial stage of an experimental study, it is frustrating to have to spend considerable time on its production when the impression gained from the literature is that it is a relatively straightforward process. The present paper is therefore an attempt to clarify the situation by discussing the various differences and difficulties in previous work (particularly concerning the approximations made by Lau & Baines 1968). Numerical solutions are presented, the sizes of the neglected terms implicit in the analysis are indicated and comparisons are made with careful experimental measurements, thus demonstrating the limitations of the theory.

2. The analysis

The basic analysis presented by previous authors will not be restated in detail; we emphasize merely the differences in approach and the main assumptions and results.

For two-dimensional, inviscid, incompressible flow the vorticity equation can be written as

$$\omega \equiv \partial v/\partial x - \partial u/\partial y \equiv \nabla^2\psi = \rho^{-1}\, dH/d\psi = f(\psi) \tag{1}$$

in the usual notation and where $H = P + \frac{1}{2}\rho(u^2+v^2)$. In the particular case of a uniform upstream velocity and a prescribed linear variation in the downstream velocity $f(\psi)$ takes particularly simple forms and (1) can be solved directly without any assumptions concerning streamline displacements. This was the approach adopted by Lau & Baines (1968), who also included the effect of density gradients. To obtain a complete solution of the flow through the screen it is necessary to match the upstream and downstream solutions of (1) by formulating suitable gauze boundary conditions. By making gross assumptions about one of the boundary conditions Lau & Baines (1968) were able to

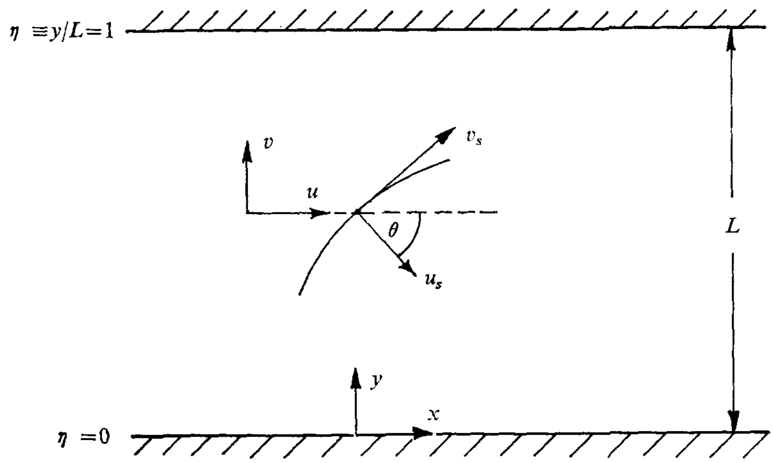

FIGURE 1. Definition diagram. Suffixes 1 and 2 refer to conditions upstream and downstream of the gauze, respectively.

take the streamline deflexion into account. Alternatively the streamline deflexions may be assumed to be small so that the solution of (1) becomes identical to the solution of the perturbation stream-function equation obtained by assuming small transverse displacements:

$$\nabla^2\psi^* = 0, \tag{2}$$

where ψ^* is defined by $\psi = \psi_0 + \psi^*$ and ψ_0 is the stream function far upstream (or downstream). For more general $f(\psi)$ in (1) it is necessary to solve (2), and this was Elder's (1959) approach.

Mass continuity through the gauze leads directly to the first boundary condition, which is

$$u_1 = u_2 + (v_1 - v_2)\,T, \tag{3}$$

where $T = \tan\theta$ and figure 1 defines the notation.

The screen also experiences a lift force, so that $v_{s1} \neq v_{s2}$. It is usual to define a deflexion coefficient B as

$$B = (v_{s1} - v_{s2})/v_{s1} = g(K, \theta),$$

where K is the gauze resistance coefficient, defined by $K = \Delta p/\tfrac{1}{2}\rho u_s^2$, and Δp is the pressure drop across the gauze. On the basis of the evidence of Davis (1957), which suggests only a weak dependence on θ, all previous authors have assumed that B is not a function of θ. Progress without this assumption is extremely difficult but it is important to recognize that it *is* an assumption and in fact this, together with the difficulty of actually assigning a value for B, seems to be a major problem in using the theory and is discussed further in § 4. The second boundary condition becomes, using (3),

$$Bu_1T = (1-B)\,v_1 - v_2 + (v_1 - v_2)\,T^2. \tag{4}$$

Both Elder (1959) and Lau & Baines (1968) neglect the term $(v_1 - v_2)\,T$ in (3) and the term $(v_1 - v_2)\,T^2$ in (4), a process which, as they recognize, is valid only if T is small. Lau & Baines (1968) also drop the term Bu_1T in (4) arguing that "the streamline pattern for the present case is much the same as if a screen normal to the flow is used to deflect the streamlines into the required downstream pattern". They state that "the errors involved...will not be serious if the inclination of the screen, and hence T, is small". However, if T is small, v_1 and v_2 will be small and in fact it seems probable that T, v_1 and v_2 are all quantities that are small to first order, so it is unreasonable to drop Bu_1T whilst retaining $(1-B)v_1$ and v_2 in (4). It is shown in § 3 that this assumption of Lau & Baines (1968) leads to considerable divergence from the theory of Elder.

The third boundary condition can be obtained either from the inviscid equation of motion

$$\rho^{-1}\nabla H = \mathbf{U}\times\boldsymbol{\omega},$$

which leads to

$$\rho^{-1}\partial(\Delta H)/\partial y = -u_1\partial u_{-\infty}/\partial y + u_2\partial u_{+\infty}/\partial y, \tag{5}$$

where

$$\Delta H = H_1 - H_2 = \Delta p + \tfrac{1}{2}\rho(v_{s1}^2 - v_{s2}^2)$$

(Elder 1959), or by equating the energy change along a streamline with the energy loss ΔH at the screen. This was the procedure adopted by Lau & Baines (1968) and leads to

$$\rho^{-1}\Delta H = \tfrac{1}{2}u_{-\infty}^2 - \tfrac{1}{2}u_{+\infty}^2 + \rho^{-1}(\Delta p)_T, \tag{6}$$

where $(\Delta p)_T$ is the static pressure drop from far upstream to far downstream (which is independent of y) and

$$\Delta H = \tfrac{1}{2}\rho\cos^2\theta\{Ku_1^2 + (v_1^2 - v_2^2)\}. \tag{7}$$

Since they eliminated the gauze inclination from the first two boundary conditions (3) and (4), Lau & Baines (1968) were able to solve (1) with (3) and (4) to obtain u_1, v_1, u_2 and v_2, and hence find the variation of $\cos^2\theta$ directly from (6) and (7). This necessitated fixing $\rho^{-1}(\Delta p)_T$, which they did by specifying the gauze slope as zero at one of the walls ($y = 0$) to satisfy the deflexion equation (4). However, it is immediately obvious that the problem is now over-simplified since it should be equally correct to specify the gauze slope as zero at the other wall ($y = L$). Calculations show that even for small shear the solutions are very different (see § 3).

A less arbitrary approach was adopted by Elder (1959), who linearized $\cos^2\theta$ by writing

$$\gamma = K\cos^2\theta = \gamma_0(1+s),$$

where γ_0 is a constant given by

$$\gamma_0 = \int_0^1 K\cos^2\theta\, d\eta$$

and s is much less than unity.

Equation (5) can now be integrated to give

$$u_{-\infty} - u_{+\infty} = \gamma_0(q-1) + \tfrac{1}{2}\gamma_0 s, \tag{8a}$$

where $u_1 = u_2 = q$ (the approximated first boundary condition) and second-order terms have been neglected. The standard solution of (2) (e.g. Elder 1959) together with (8a) and the approximated second boundary condition, i.e.

$Bu_1T = (1-B)v_1 - v_2$, lead to

$$BTq = \sum_n \alpha_n \sin n\pi\eta \tag{8b}$$

and
$$u_{+\infty} - q + (1-B)(u_{-\infty} - q) = \sum_n \alpha_n \cos n\pi\eta, \tag{8c}$$

where the α_n are constants to be determined. Elder (1959) was able to solve (8) analytically for particular variations of gauze inclination (a linear and a parabolic gauze). The case of more practical interest, the θ distribution required for a specified linear downstream shear, is different in that s is neither zero nor specified and γ_0 is not known. As Turner (1969) pointed out, the equations must be solved by a numerical iterative technique. The first iteration is performed with $\gamma_0 = K$ and $s = 0$. This is in fact equivalent to Elder's analytic solution of (8) for a linear shear profile but he appears not to have realized that it is not the correct solution, in which s must be non-zero. Actually, there is an error in Elder's analysis, so that even this 'first iteration' is not correct. Lau & Baines (1968) correct this error (but see appendix B), as does Maull (1969). Equations (8) imply an asymmetric variation of $\tan\theta$ about the tunnel centre-line for non-zero s and this indicates a difficulty in Turner's (1969) paper, in which, although he describes a correct procedure for a numerical solution, his plotted screen shapes are antisymmetric and in fact he states that "the computed gauze shape is practically unchanged if the resistance variation term $s(\omega)$ is neglected". This is in disagreement with the present work and that of Livesey & Laws (1973) and Chan (1971). Maull (1969) found experimentally that the $s = 0$ solution did not produce a good linear shear profile and he had to adjust the gauze shape empirically. The final shape was, as might be expected, not antisymmetric about the tunnel centre-line.

3. The neglected terms

Initial results of a numerical solution of (8) did not agree with the results given by Turner (1969) and it was this that actually prompted a closer investigation of the whole problem. The numerical procedure (with its associated difficulties) used in the present study is outlined in appendix A and will not be discussed here, except for the comment that for the purposes of comparison all solutions were obtained with a deflexion coefficient B given by

$$B = 1 - (1 + \sqrt{K})^{-\frac{1}{2}}$$

in common with previous workers. The practical validity of this relation is discussed in § 4, where experimental results are considered.

A measure of the differing results in the literature is shown in figure 2. The author's numerical solution of (8) for $K = 4{\cdot}2$ and $\lambda = 0{\cdot}5$, where λ is the shear, defined by

$$u_{+\infty} = u_{-\infty} + \lambda(\eta - \tfrac{1}{2}), \tag{9}$$

is compared with results of previous workers.

It was initially thought that for small values of λ the theories of Elder (1959) and Lau & Baines (1968) would give similar results as, presumably, the various

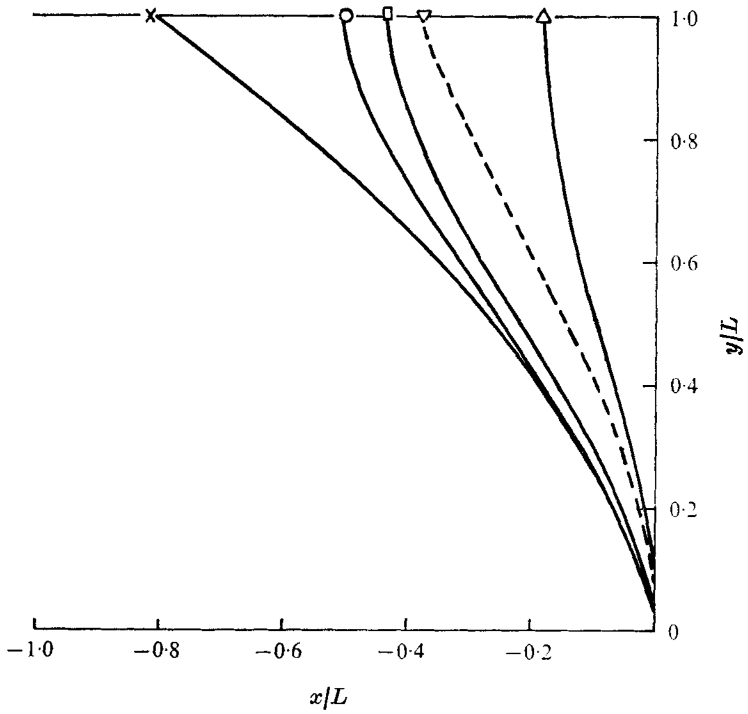

FIGURE 2. The gauze shape required for $\lambda = 0{\cdot}5$, $K = 4{\cdot}2$. Previously published results compared with the author's numerical solution using Elder's (1959) theory. ×, Lau & Baines' (1968) theory; △, Turner's (1969) numerical solution of (8); ○, the 'first iteration' ($s = 0$) solution (appendix B or Maull 1969); □, Lau & Baines' (1968) plot of the 'first iteration' solution; ▽, the author's numerical solution of (8) (Elder's theory).

approximations become less important. Figure 3 shows a comparison between the two theories for $K = 2{\cdot}0$ and $\lambda = 0{\cdot}05$. The numerical solution of (8) (Elder's equations) is used (with $s \neq 0$) although of course for this case the 'first iteration' ($s = 0$) solution is almost identical with the final solution since λ is very small. It is apparent that there is a considerable difference between the two theories. As stated in § 2, Lau & Baines could equally have satisfied the deflexion equation at the top wall rather than the bottom one and the resulting profile is included in figure 3. Section 2 indicates that the neglect of the term Bu_1T in the second boundary condition (4) is likely to be invalid, so for the Lau & Baines (1968) solution this term was computed and compared with one of the remaining terms (v_2). The results for various values of λ are shown in figure 4. It is clear that even for small shear Bu_1T is an order of magnitude larger than v_2 (or $(1-B)v_1$) and in fact as λ decreases Bu_1T/v_2 actually increases. The second boundary condition is therefore strongly violated and it is this that causes the very different result obtained by Lau & Baines.

By contrast, the other terms neglected by both Elder (1959) and Lau & Baines (1968) in the boundary conditions are all small for small values of λ, but in order to investigate the probable range of validity of the theory it is necessary to estimate the size of these neglected terms.

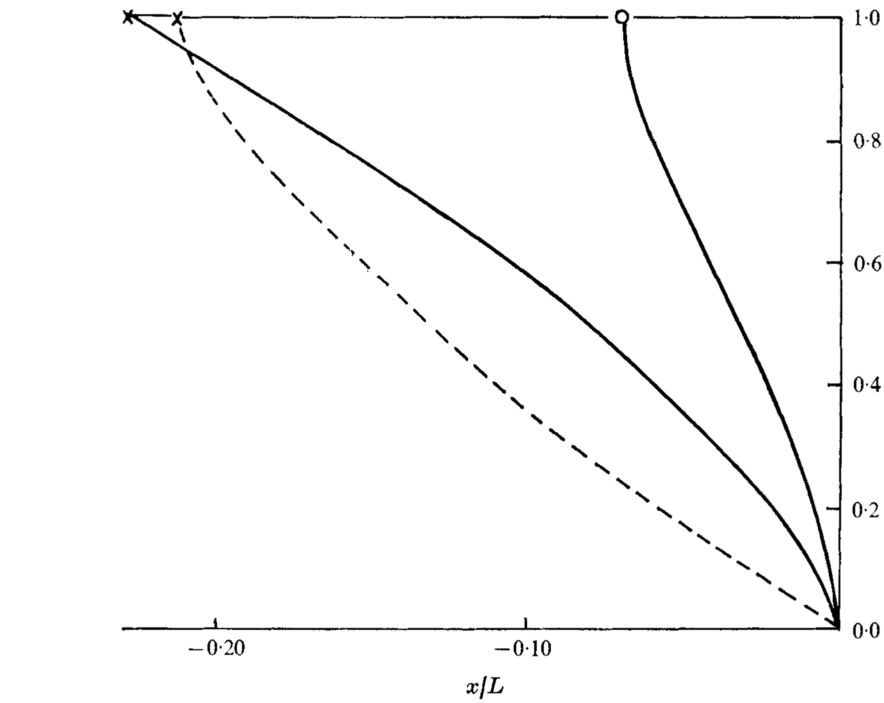

FIGURE 3. Comparison between the theories of Lau & Baines (1968) and Elder (1959) for low shear. $\lambda = 0{\cdot}05$, $K = 2$. ○, Elder; ×, Lau & Baines; ——, gauze slope zero at $\eta = 0$; – – –, gauze slope zero at $\eta = 1$.

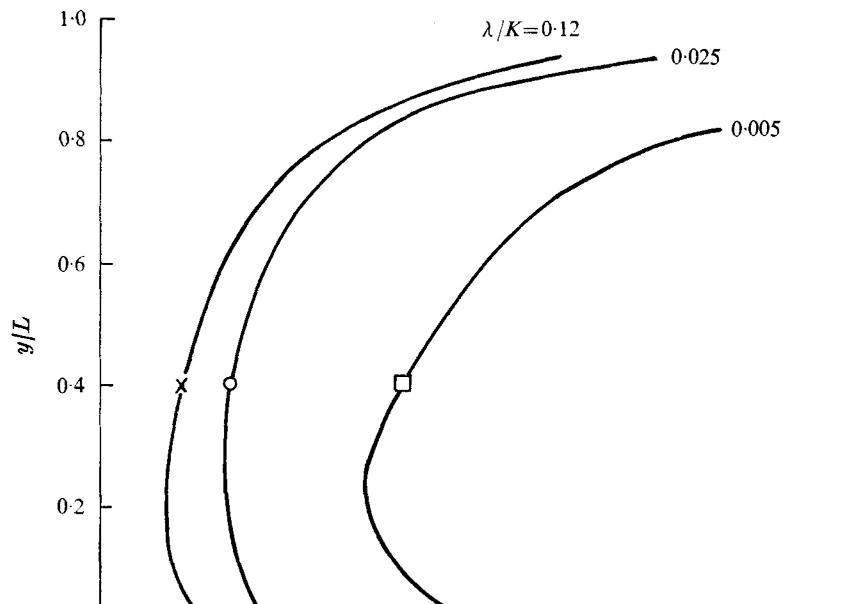

FIGURE 4. The term neglected by Lau & Baines in the second boundary condition (4). ×, $\lambda = 0{\cdot}5$, $K = 4{\cdot}2$; ○, $\lambda = 0{\cdot}05$, $K = 2$; □, $\lambda = 0{\cdot}01$, $K = 2$.

The most stringent requirement in the approximation of the gauze boundary conditions is that

$$(v_1 - v_2)T \ll B,$$

where the velocity at the gauze has been taken as unity for convenience. For a linear downstream shear profile, defined by (9), it can be shown, by a consideration of the basic solution of (2), that

$$v_1 + v_2 = 4\lambda a/\pi^2 = a', \quad \text{say}, \tag{10}$$

where a is given by

$$a = \sum_{n\ \mathrm{odd}}^{\infty} (\sin n\pi\eta)/n^2.$$

Manipulation of the approximated second boundary condition, i.e.

$$(1-B)v_1 - v_2 = Bu_1T \simeq BT,$$

with (10) leads to

$$(v_1 - v_2)T/B = \{T/(2-B)\}(a' + 2T). \tag{11}$$

We need to have an estimate of $\tan\theta$ before it is possible to estimate the size of the right-hand side of (11). A reasonable approximation is provided by the 'first iteration' ($s = 0$) solution, for which an analytic expression is available for $\tan\theta$. This can be deduced quite simply (e.g. Maull 1969) and is given by

$$T = \frac{-4\lambda}{\pi^2 EB} \sum_{n\ \mathrm{odd}}^{\infty} (\sin n\pi\eta)/n^2 = -a'/EB, \tag{12}$$

where

$$E = K/(2+K-B).$$

Hence

$$\epsilon \equiv \{(v_1 - v_2)T/B\} = (2/EB - 1)a'^2/\{EB(2-B)\}. \tag{13}$$

It is worth noting that, since EB is usually significantly less than unity, ϵ can be written as

$$\epsilon \sim (\lambda/EB)^2(2-B)^{-1}\,C(\eta) \quad \text{to first order.}$$

Now

$$\lambda/EB = (\lambda/K)(2+K-B)/B$$

and, since $(2-K-B)/B$ is only a weak function of K in the range of practical interest, the dominant parameter is seen to be λ/K. Livesey & Laws have in fact, in another paper (1972), pointed out that given a required downstream velocity profile only a certain range of screen parameters will admit a real solution: if λ/K is too large there is no real solution. This is considered further in appendix A, where the problems encountered in numerical solution of (8) are briefly discussed.

Given the gauze parameters and the shear parameter λ, (13) gives an estimate of the largest term neglected in the boundary conditions. It is a straightforward, though lengthy, process to show that the sum of the terms neglected in the ΔH term of the third boundary condition [(5) or (6)] is considerably smaller than ϵ. ϵ is plotted against λ in figure 5 for $K = 1$ and $K = 4$. Only the centre-line ($\eta = \frac{1}{2}$) values are included and it is obvious that even with a high resistance screen ϵ becomes quite large for moderate values of λ. As a check that (13)

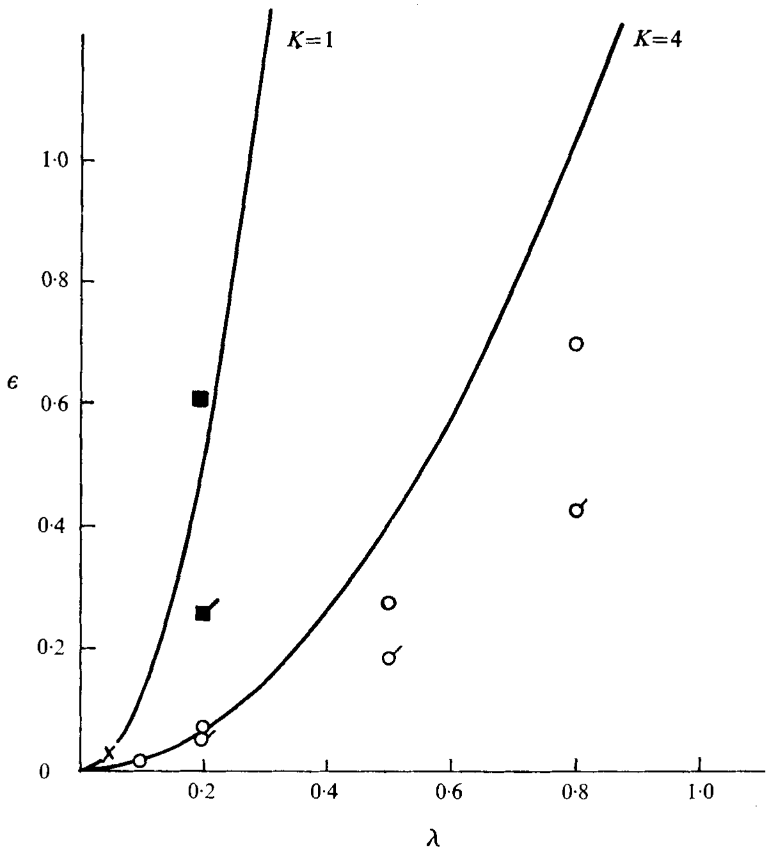

FIGURE 5. Values of the largest neglected term in the boundary conditions. ——, ϵ as given by (13) at $\eta = 0{\cdot}5$; unflagged symbols, maximum values of ϵ computed from results of the numerical solution ($s \neq 0$); flagged symbols, values of ϵ at $\eta = 0{\cdot}5$; ■, $K = 1$; ○, $K = 4$.

adequately represents the size of the neglected term the exact values of $(v_1 - v_2)T/Bq$ were computed, using the final iterated values of $\tan\theta$, and typical results are included in figure 5. As anticipated, (13) over-estimates the error on the centre-line but is in fact reasonably representative of the maximum value of the error term (which occurs at about $\eta = 0{\cdot}75$ in most cases). For small values of λ, of course, there is close agreement as the final value of T is not very different from the 'first iteration' ($s = 0$) value.

It is also instructive to note the values taken by v_1 and v_2. Although the results will not be presented in detail it can be shown that the total streamline deflexion is relatively small, so the assumption of small streamline deflexion is valid over a somewhat wider range of λ/K than are the approximations made in the boundary conditions, particularly in (4).

We conclude that for low values of λ/K (less than 0·1 say) there is no reason to doubt that Elder's theory should give good results but at higher values of λ/K the approximations become increasingly invalid. The experimental work described in the following section confirms these expectations, particularly that at large λ/K the theory is inaccurate, a finding which agrees with that of Chan (1971).

4. Experimental comparisons

Many of the authors mentioned previously made comparisons between their various solutions and experimental results but meaningful comparisons are difficult for at least two reasons. First, it has been shown by various authors (e.g. Jackson 1972) that small variations in wire-gauze parameters (wire diameter and mesh size) produce significant inhomogeneities in the downstream velocity profile. Usually this is not a problem as smoothing screens are often mounted upstream of a contraction, but curved gauzes for producing linear shear profiles are invariably mounted in the working section. Since the turbulence levels are very low there is no effective mechanism for reducing the inhomogeneities, which therefore persist for a considerable distance downstream. For values of the screen coefficient K greater than about 2 (corresponding to open-area ratios less than about 0·5) a particularly serious form of velocity inhomogeneity arises owing to an instability of the flow through the screen, usually termed 'jet coalescence' (Baines & Peterson 1951; Bradshaw 1965). Unless measurements are made at small intervals of η, such inhomogeneities can be easily overlooked; however, if closely spaced measurements are made there is usually considerable scatter, which may only amount to, say, 2 % of the centre-line velocity but can be significant compared with the total variation across the working section. Inspection of the literature shows that where sufficient measurements have been made there is significant scatter and this makes it difficult to draw definite conclusions about the magnitude of the shear developed by the gauze. The present measurements are somewhat similar in this respect.

A second difficulty associated with experimental comparisons concerns the value of the deflexion coefficient B. Following Elder (1959) and Turner (1969) the numerical solutions described in § 3 used the relation

$$B = 1-(1+\sqrt{K})^{-\frac{1}{2}}, \tag{14}$$

which is similar to the relation proposed by Taylor & Batchelor (1949):

$$B = 1-1\cdot1(1+K)^{-\frac{1}{2}}. \tag{15}$$

However, it appears that, for their experimental comparisons, most previous workers used values of B significantly less than those given by either of the above relationships. For example Elder himself states that he used a screen with $K = 2\cdot20$ and $B = 0\cdot22$, compared with the values of $B = 0\cdot365$ and $B = 0\cdot385$ which (14) and (15) would respectively give. Davis (1957) shows that measured values of B are almost always less than those given by (14) and (15) but are very scattered, although B seems to decrease slightly with K. The actual measurement of B is not simple, and for the purposes of the present work the screen shapes were calculated using (14). It is of course a fairly simple matter to deduce the downstream velocity profiles for different values of B.

Gauze	SWG	Wire diameter d (in.)	Meshes/ in., m	Open-area ratio $\beta = (1-md)^2$	K_{100}	K_{15}
I	33	0·010	30	0·490	2·33	1·84
II	29	0·0136	28	0·362	4·92	3·68
III	29	0·0136	18	0·570	1·55	1·16

TABLE 1. K_{100} is defined as the resistance coefficient at a Reynolds number (based on wire diameter) of 100, as given by *Royal Aeronautical Society Data Sheet* no. 02.00.01 (1963). K_{15} is the resistance coefficient at a stream velocity of 15 m/s, also deduced from the above reference.

All the experiments were done in a channel with an approximately 250 mm square cross-section mounted in an open-return wind tunnel with a (closed) working section of $0{\cdot}27 \times 0{\cdot}91 \times 10$ m. The upstream 500 mm portion of this channel was specially made for each curved screen used. This arrangement obviated the necessity of adding a completely new working section to the existing wind tunnel for each screen investigated. The screens were soldered to brass formers mounted outside the channel. It was found necessary to apply considerable side tension to ensure the correct gauze shape all across the channel and this was done by simply tightening bolts passed through one of the formers and bearing externally on the channel walls. Checks with a shaped template indicated that, even for the most highly curved screen, deviations from the required shape were everywhere less than $\frac{1}{2}$ mm. Velocity measurements were made with small round-nosed Pitot tubes and standard manometers. Checks on the upstream velocity profile showed that the deviation from uniformity was less than $\frac{1}{4}$ % except in the wall boundary layers, which were less than 5 % of the channel height in thickness. The downstream velocity measurements were all made at least one channel height (about 700 wire diameters in the worst case) and in most cases two channel heights downstream from the screen.

Royal Aeronautical Society Data Sheet no. 02.00.01 (1963) gives the values of open-area ratios β and consequent screen resistance coefficients K for a variety of typical screens at various Reynolds numbers Re_d. A single test with a 30/33 SWG screen (see table 1) gave a value of K within 2% of that given by the *Data Sheet*. This may have been somewhat fortuitous, but it was not felt worth while to undertake an exhaustive investigation since the exact value of K is not too critical. Indeed for the first test case of a low shear ($\lambda = 0{\cdot}10$) a change of 20 % in K changes the calculated downstream extent of the gauze by about 3 mm. Table 1 gives the relevant details of the various screens used. Because there is a variation of K with Reynolds number, all the values of K were evaluated for a free-stream velocity of 15 m/s (corresponding to wire Reynolds numbers between about 250 and 350) and all the tests were performed at this velocity.

For the case of linear downstream shear there has been no adequate demonstration that Elder's theory is applicable even for low shear, although the considerations in § 3 suggest no reason why it should fail. This was the first

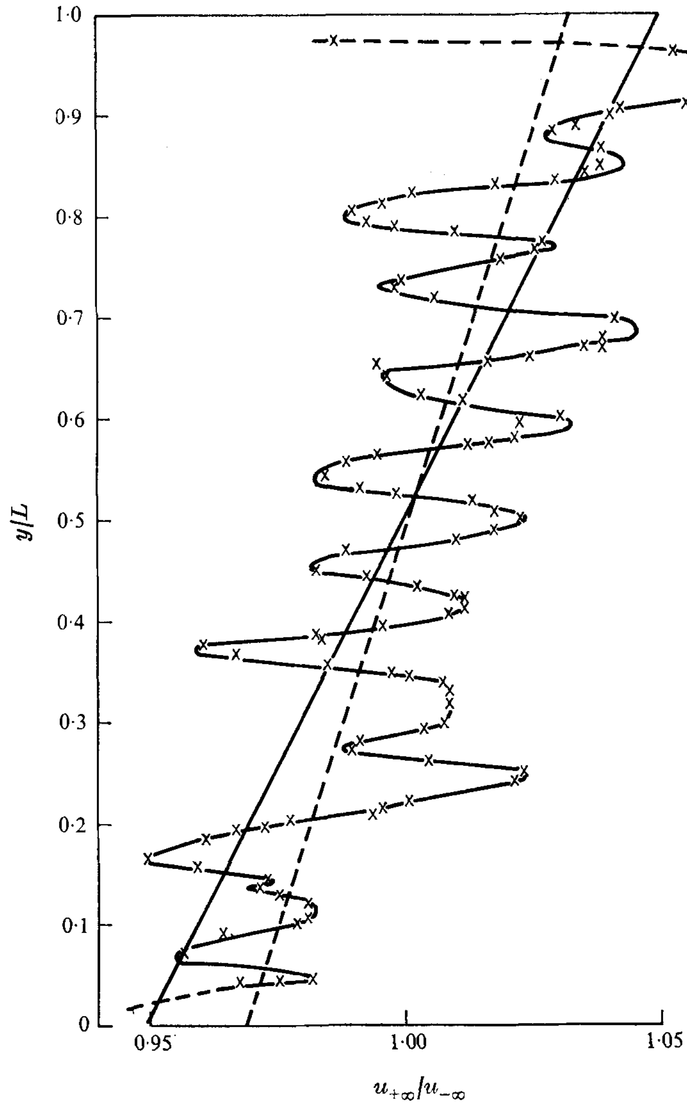

FIGURE 6. Velocity variation downstream of gauze I ($K = 1{\cdot}84$) shaped to give $\lambda = 0{\cdot}1$ (with $B = 0{\cdot}35$, equation 14). ×, measurements; ——, required $\lambda = 0{\cdot}1$ profile; – – –, theoretical profile for $B = 0{\cdot}2$.

objective of the experimental programme. The gauze shape required to produce a linear shear defined by

$$u_\infty - 1 = \lambda(\eta - \tfrac{1}{2})$$

with $\lambda = 0{\cdot}1$ was computed for a screen with a resistance coefficient K of 1·84 (gauze I in table 1). For this case, of course, inclusion of the s term (see § 3) made only a small difference to the required gauze shape.

Figure 6 shows the downstream velocity profile actually generated by the gauze and it is immediately obvious that jet coalescence has occurred. It is clearly almost impossible to determine the actual shear developed, although a

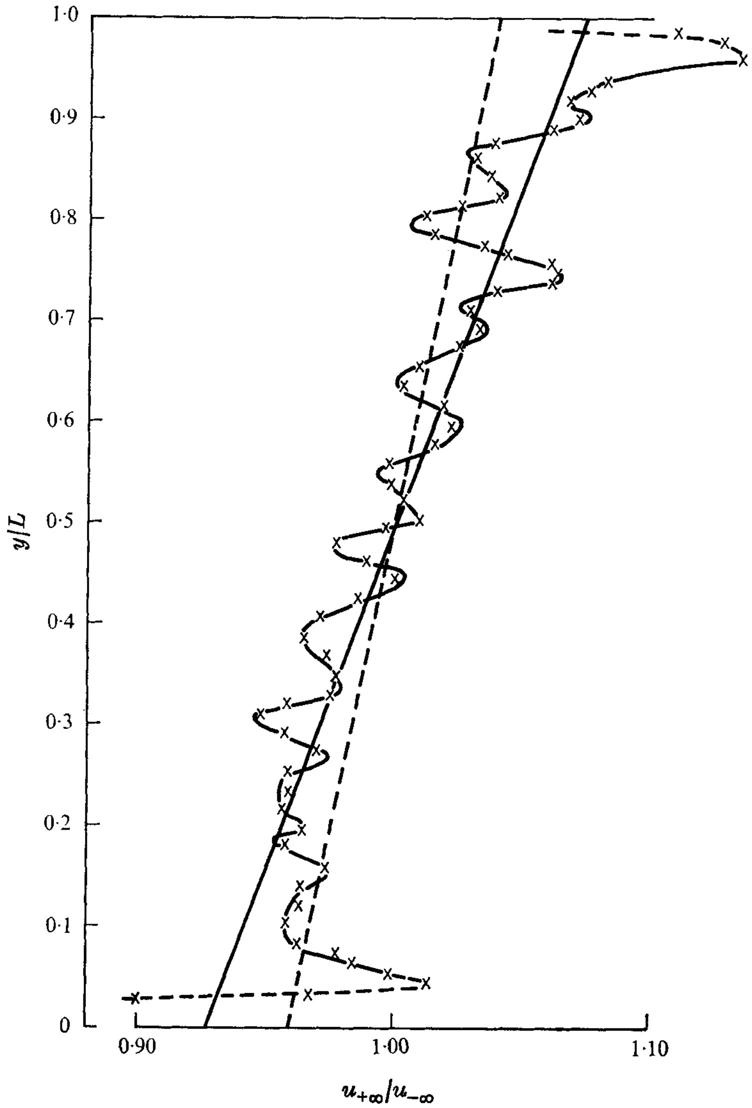

FIGURE 7. Velocity variation downstream of gauze II ($K = 3{\cdot}68$). ×, measurements; ——, theoretical profile for $B = 0{\cdot}415$ [equation (14)]; – – –, theoretical profile for $B = 0{\cdot}2$.

least-squares fit would show the velocity profile to be slightly closer to the line representing the calculated downstream profile for $B = 0{\cdot}2$ than to the $\lambda = 0{\cdot}1$ profile [corresponding to the B calculated from (14)].

Gauze II ($K = 3{\cdot}68$) was fitted to the same formers and the resulting downstream velocity is shown in figure 7 compared with the velocity variations (not, of course, exactly linear in this case) computed using B from (14) and $B = 0{\cdot}20$. Again it seems that there is some jet coalescence although in this case the agreement is better for B calculated from (14). It is interesting to note that in the region of the wall boundary layers there is a considerable velocity excess. This effect was noted by Owen & Zienkiewicz (1957) and Livesey & Turner

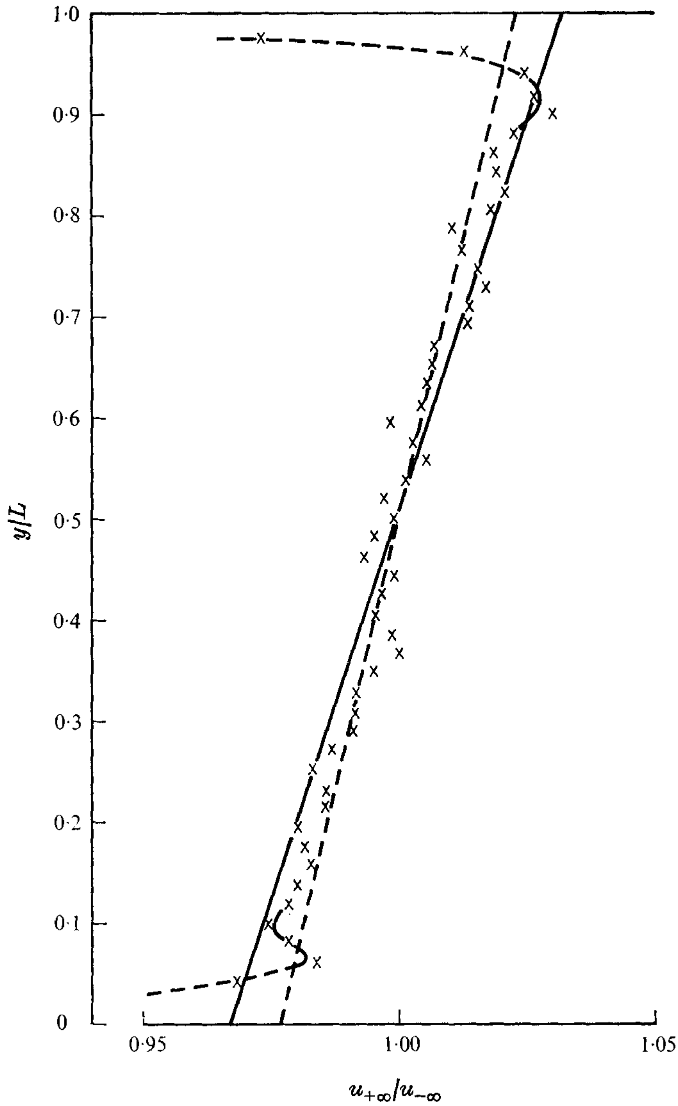

FIGURE 8. Velocity variation downstream of gauze III ($K = 1{\cdot}16$). ×, measurements; ——, theoretical profile for $B = 0{\cdot}306$ [equation (14)]; – – –, theoretical profile for $B = 0{\cdot}2$.

(1964) (for a grid of rods) and by Lau & Baines (1968) (for a screen), who showed that for $K > 1$ the kinetic energy in the outer part of the boundary layer will tend to increase with distance from the wall since the boundary-layer fluid suffers a smaller loss in total head than the fluid outside when passing through the screen. For K values less than about 2·0 there should be no jet coalescence, so gauze III ($K = 1{\cdot}16$) was next fitted to the same formers. The resulting velocity profile is shown in figure 8. There is a scatter of, at most, 1 % of the mean velocity and this is probably caused by screen inhomogeneities. However, within the experimental accuracy the agreement is satisfactory and would

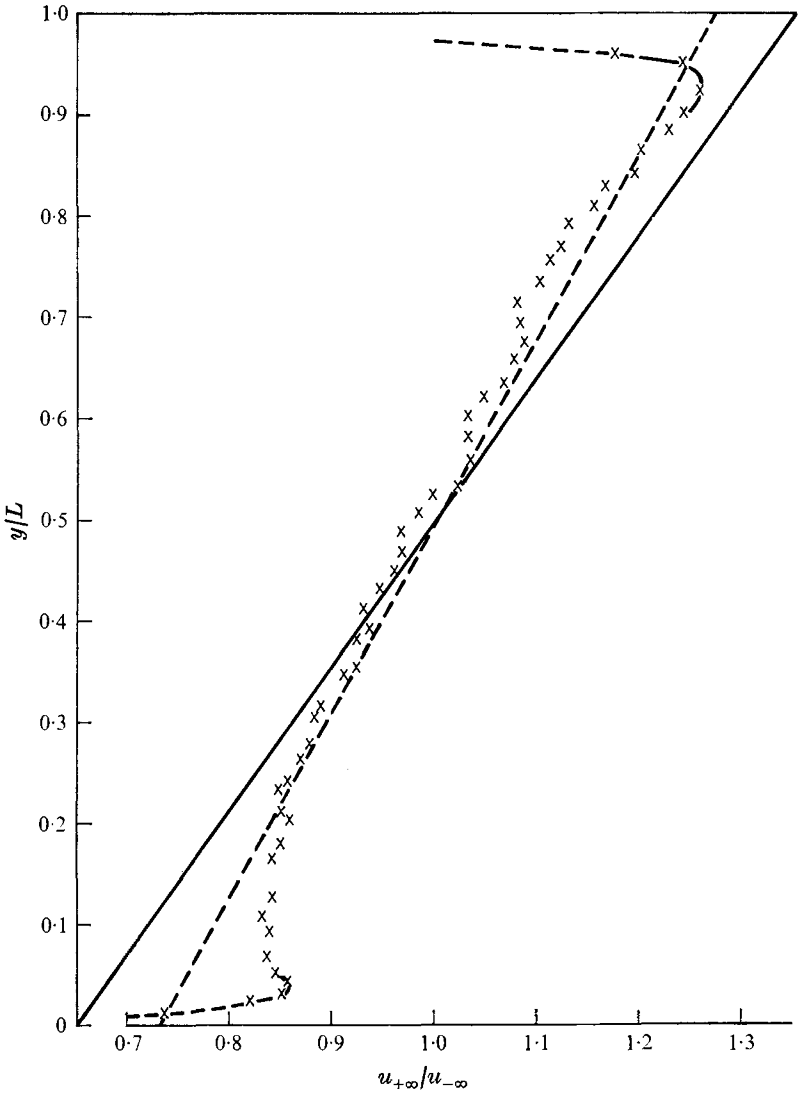

FIGURE 9. Velocity variation downstream of gauze II (K = 3·68) shaped to give λ = 0·7 [with B = 0·415, equation (14)]. ×, measurements; ——, required λ = 0·7 profile; – – –, theoretical profile for B = 0·2.

be best for a value of B somewhere between 0·2 and the value calculated from (14).

These results highlight the problems discussed previously, but encourage one to believe that the theory is satisfactory for low shears, as was expected. In practice, of course, substantially higher values of λ are usually required and the second stage of the experimental programme was designed to test the theory for a typical high value of the shear. Gauze II (K = 3·68) was fitted in the channel to the shape required by the theory to give a linear shear profile defined by λ = 0·70 and in this case inclusion of the s term was necessary (but see § 5). The velocity profile produced by this gauze is shown in figure 9.

Although, since $K > 2$, there is probably some jet coalescence, it is not serious as the shear developed is relatively large. The scatter is, in fact, about 2 % of the centre-line mean velocity, which is comparable with that shown in figure 7. Clearly the required shear ($\lambda = 0{\cdot}70$) has not been produced and the profile is only roughly linear over the central 70 % of the channel. Agreement with the theoretical velocity profile calculated for $B = 0{\cdot}2$ is somewhat better, but the results shown in figure 7 suggest that this is an unlikely value for the deflexion coefficient for gauze II ($K = 3{\cdot}68$). It seems more probable that the theory becomes inadequate for such a large value of λ. This inadequacy is more clearly demonstrated in figure 10, which shows the velocity profile generated by gauze II ($K = 1{\cdot}16$) fitted to the same formers as were used for the previous case. Although the profile is reasonably linear it is very different from the computed profile, even with $B = 0{\cdot}2$. To force any agreement would require a B value substantially less than 0·2, which, as shown in figure 8, is highly unlikely. It is just possible that the lift coefficient may be a strong function of gauze inclination. However, Davis (1957) found experimentally that for angles of incidence up to at least 25° the deflexion coefficient is almost constant. On the other hand, there was no direct relation between B and K, which there would be if B were a function of wire diameter and spacing only, so that either B depends on some additional screen parameter (like the 'ripple' in the wires) or variations in manufacture from screen to screen affect B much more severely than K. The difficulty of deciding the proper value (or variation) of B is certainly a severe problem in any application of the theory, but the most likely reason for the large discrepancies between theory and experiment shown in figures 9 and 10 is simply that, as anticipated in § 3, the theory breaks down at high values of λ.

5. Discussion and concluding remarks

As stated in § 3, Elder (1959) 'linearized' the $\cos^2\theta$ occurring in the ΔH in (5) by writing

$$\gamma = K\cos^2\theta = \gamma_0(1+s).$$

Now Livesey & Laws (1973) have correctly pointed out that s is in fact a second-order term in θ, so that the correct first-order solution should not include it. On that basis they omit the s term altogether and apparently achieve better experimental agreement even for a highly curved screen. Their conclusion, which is unfortunately confused by some analytical errors and a downstream velocity profile that fails to satisfy continuity, was that "the discrepancy between theory and experiment...has been shown to be attributable to the inclusion of a second-order term in the essentially first-order theory". But in the case of a linear downstream velocity profile, Maull (1969) clearly demonstrated that the $s = 0$ (first-order) theory was not adequate for large shear. For a highly curved screen the s term is of similar magnitude to the other terms (as Livesey & Laws explicitly state) so in principle it should be included in any comparison with experiment. However, as shown in § 3, the approximations made in the gauze

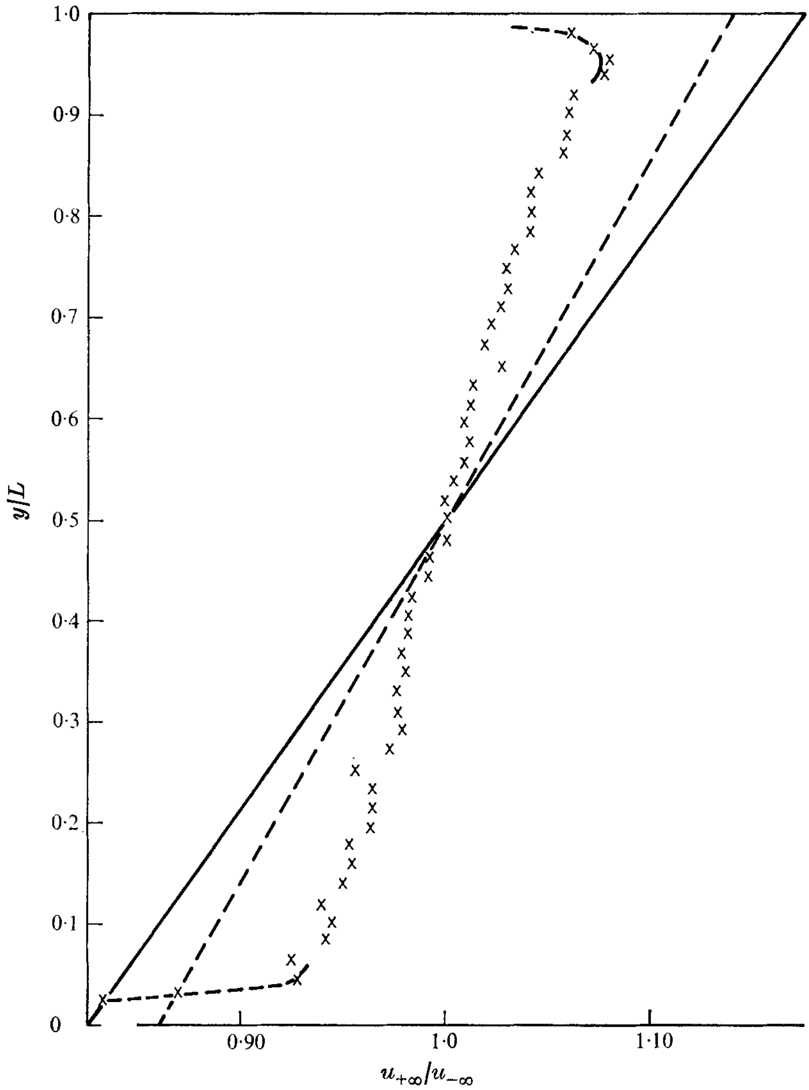

FIGURE 10. Velocity variation downstream of gauze II ($K = 1{\cdot}16$). ×, measurements; ——, theoretical profile for $B = 0{\cdot}306$ [equation (14)]; – – –, theoretical profile for $B = 0{\cdot}2$.

boundary conditions lead to errors which are, in fact, larger than the s term itself for only moderate screen inclinations, so that these other neglected terms should also be included. It is in this sense that a solution including only the s term is a 'pseudo' second-order solution. The present experimental results confirm that including the s term alone is not sufficient. Its effect is to reduce the gauze inclination (figure 2) whereas the experiments indicate that for large shear the screen is not curved sufficiently to develop the required velocity profile (figure 10). Neglecting the s term could quite possibly improve the agreement with experiment in certain cases as the work of Livesey & Laws (1973) seems to show, but this would be entirely fortuitous and is in no way a better theoretical approach for the case of high screen curvature.†

We have tried to include some of the neglected terms in the numerical solution but, for reasons which are rather obscure, this appeared to be very difficult. A more thorough attack on a full second-order solution would possibly be successful, but for the reason given below there is no guarantee that this would yield better agreement with experiment and we do not feel it to be worth while. What is clear is that the basic first-order solution can only properly be applied for relatively low values of the shear parameter λ (more strictly λ/K) and there is no simple way of improving the situation. This is unfortunate since it considerably reduces the usefulness of the theory at least for the common practical case of relatively large linear shear.

In addition to this fundamental theoretical limitation there is the practical difficulty of the deflexion coefficient B discussed in § 4. Even if an accurate second-order solution could be obtained there would still be considerable uncertainty about the proper value of B. Indeed, particularly for a highly curved screen, there is a distinct possibility that B should vary over the height of the screen and this would make the formulation of even a first-order solution much more difficult. It would appear therefore that the use of curved gauzes for the production of linear shear profiles is somewhat limited; one is reduced to using the theory as a first guess (preferably with $s = 0$) and then either accepting the resulting profile if it is linear over a usable range, or adjusting the shape empirically as Maull (1969) did. In general, the shear developed will be considerably smaller than anticipated, even if the s term is excluded from the calculations.

Since there are also bound to be inhomogeneities of at least 1 % in the resulting profile, even if a 'high-tolerance' screen material is used, it seems that there is a good case for seeking an alternative technique for producing linear shear flows. One promising method has been described by Kotansky (1966) and was used (in conjunction with grids) by Rose (1970) in his studies of the structure of a homogeneous turbulent shear flow. However, further work is required to demonstrate that the method, which involves shaping a block of honeycomb, is capable of producing a high shear with very low turbulence levels.

This work was undertaken at the Marchwood Engineering Laboratories of the Central Electricity Generating Board and is published by kind permission of the Director. Thanks are also due to Dr A. G. Robins for several helpful comments during the course of the work, to Mr E. Day, who successfully overcame the practical problems of mounting curved gauzes, and to the referees, who made several helpful suggestions.

† A referee has inquired about the agreement between the theory and experiment of Lau & Baines (1968); the above considerations seem to provide an explanation. Figure 2 shows that their neglect of an important term in the second boundary condition (discussed in § 3) leads to gauze shapes somewhat more curved than Elder's theory suggests even without the s term. A somewhat coincidental agreement with experiment is then quite possible.

Appendix A. The numerical solution of (8)

For convenience we re-state the equations to be solved:

$$BTq = \sum_1^\infty \alpha_n \sin n\pi\eta, \tag{A1}$$

$$u_{+\infty} - q + (1-B)(u_{-\infty} - q) = \sum_1^\infty \alpha_n \cos n\pi\eta, \tag{A2}$$

$$u_{-\infty} - u_{+\infty} = \gamma_0(q-1) + \tfrac{1}{2}\gamma_0 s. \tag{A3}$$

Turner (1969) outlined the procedure for solving these equations but, in common with Livesey & Laws (1972) and Chan (1971), the present author found initial difficulties associated with convergence of the iterative scheme and the final results do not agree with those of Turner (see figure 2) so it is worth while to describe the procedure in a little detail.

For the usual case of the gauze shape required to produce a given downstream shear profile (not necessarily linear) from a given upstream profile (not necessarily uniform), $u_{-\infty}$ and u_∞ are both known and fixed functions of η. q is found from (A3) (putting $\gamma_0 = K$ and $s = 0$ for the first iteration) and the left-hand side of (A2) is computed:

$$F(\eta) = u_\infty - q + (1-B)(u_{-\infty} - q).$$

In order to determine the coefficients α_n, $F(\eta)$ is written as a Fourier cosine series; i.e.

$$F(\eta) = \frac{1}{\pi}\int_0^\pi F(\zeta)\,d\zeta + \frac{2}{\pi}\sum_n\left\{\cos n\zeta \int_0^\pi F(\zeta)\cos n\zeta\,d\zeta\right\}$$

($\zeta = \pi\eta$). Continuity requires that

$$\frac{1}{\pi}\int_0^\pi F(\zeta)\,d\zeta = 0.$$

The terms α_n are therefore given simply by

$$\alpha_n = 2\int_0^1 F(\eta)\cos n\pi\eta\,d\eta.$$

These are computed and substituted into (A1) to give BTq and hence T. Note that it is not necessary to write $q = 1$ in BTq (as do Elder 1959; Turner 1969) but the numerical results have shown that such an assumption is reasonable.

The calculation of T enables new estimates to be made of

$$\gamma_0 = \int_0^1 K\cos^2\theta\,d\eta$$

and

$$s = (K/\gamma_0)\cos^2\theta - 1,$$

and these are used in (A3) to update the values of q. The process is repeated until T (and hence γ_0) has converged. First attempts at this procedure showed that γ_0, instead of converging, oscillated and it was obvious that some form of relaxation scheme was necessary. The simplest method is to write

$$\gamma_{0i} = c\gamma_{0i} + (1-c)\gamma_{0i-1}$$

and

$$s_i = cs_i + (1-c)s_{i-1},$$

so that new values of γ_0 and s used in the next iteration are weighted by some fraction $1-c$ of the old values. This was the technique employed by Chan (1971) and it works for most cases of practical interest, provided that λ/K is not too large. In the latter case even very small values of c (0·1, say) were not sufficient to ensure stability and it appeared to be a general feature of the solution technique that if λ/K was greater than, say, 0·2 relaxation schemes were very difficult to apply successfully. As mentioned in § 3, Livesey & Laws (1972) have shown that in fact for certain screen parameters (8) only admit imaginary solutions. For example, for the case of a linear screen, $\tan\theta \equiv T =$ constant, $s = 0$, $\gamma_0 = K/(1+T^2)$ and the velocity profile is given by

$$u_\infty - 1 = (2EBT/\pi) \log \cot \tfrac{1}{2}\pi\eta, \tag{A4}$$

where

$$E = \gamma_0/(2+\gamma_0-B),$$

so specifying this downstream profile and solving the equations for $\tan\theta$ involves solving, effectively,

$$C = 2EBT/\pi = (2KBT/\pi)\{K+(2-B)(1+T^2)\}^{-1}.$$

Now (A4) is not very different from a linear shear profile defined by

$$u_\infty - 1 = \lambda(\eta - \tfrac{1}{2}),$$

where $\lambda \simeq 4C$, so real solutions for T only exist if

$$B^2K^2 \geqslant \tfrac{1}{16}(2-B)(2-B+K)\,\pi^2\lambda^2.$$

Using (14) this implies that λ/K should satisfy

$$\lambda/K \leqslant 0{\cdot}18.$$

for the usual range of K ($1 < K < 4$). So, in addition to the limit on λ/K set by the size of the error terms (§ 3) it is in fact impossible to solve the equations at all if λ/K exceeds about 0·2. This explains the increasing instability of the iterative scheme as λ/K approaches this value.

Appendix B. The analytic solution of (8) for the case $s = 0$

For the particular case of a uniform upstream flow ($u_{-\infty} = 1$) and a linear shear profile downstream, defined by $u_\infty - 1 = \lambda(\eta-\frac{1}{2})$, (8) simplify to

$$BT = \sum_n^\infty \alpha_n \sin n\pi\eta \tag{B 1}$$

and

$$(\lambda/E)\,(\eta-\tfrac{1}{2}) = \sum_n^\infty \alpha_n \cos n\pi\eta, \tag{B 2}$$

where $E = K/(2+K-B)$ and we have written $BTq = BT$; the term including the variation of resistance s has been dropped and the solution of these equations is equivalent to the first iteration in the complete numerical solution (appendix A). Elder (1959) showed that

$$T = \frac{2\lambda}{BE\pi^2}\int_0^w \log\tan\tfrac{1}{2}t\,dt \quad (w = \pi\eta)$$

but unfortunately his expansion of the integral is incorrect, as previous authors have pointed out (Maull 1969; Lau & Baines 1968). Now

$$\frac{2}{\pi}\int_0^w \log\tan\tfrac{1}{2}t\,dt = \frac{4}{\pi}\int_0^{\frac{1}{2}w}\log\tan t\,dt = I, \quad \text{say,}$$

and standard texts give

$$I = \tfrac{1}{2}w\log\tfrac{1}{2}w - \tfrac{1}{2}w + \tfrac{1}{9}(\tfrac{1}{2}w)^3 + \tfrac{7}{450}(\tfrac{1}{2}w)^5 + O(w^7)$$

provided that $0 \leqslant \frac{1}{2}w \leqslant \frac{1}{2}\pi$. In this case w never exceeds π (its value at $y = L$), so that the expansion is valid and can be integrated directly to give the gauze shape. The result is

$$x/L = (4\lambda/EB\pi^3)[\{(\tfrac{1}{2}w)^2\log\tfrac{1}{2}w\} - \{\tfrac{3}{2}(\tfrac{1}{2}w)^2\} + \{\tfrac{1}{18}(\tfrac{1}{2}w)^4\} + \{\tfrac{7}{1350}(\tfrac{1}{2}w)^6\} + O(w^8)]. \tag{B 3}$$

This is the result given by Lau & Baines (1968), except that there appears to be a printing error in their paper since $\log\frac{1}{2}w$ is written as $\log w$. Unfortunately, their plot of the gauze shape does not agree with this expression. Maull (1969) attacked the problem rather differently. He expanded $\eta - \frac{1}{2}$ as a Fourier cosine series to determine the coefficients α_n, but the result is mathematically identical to (B 3).

REFERENCES

Baines, W. D. & Peterson, E. G. 1951 *Trans. A.S.M.E.* **73**, 467.

Bradshaw, P. 1965 *J. Fluid Mech.* **22**, 679.

Chan, A. 1971 M.Sc. thesis, Imperial College, London.

Cockrell, D. I. & Lee, B. E. 1966 *J. Roy. Aero. Soc. Tech. Note*, no. 70, p. 724.

Davis, G. 1957 Ph.D. thesis, University of Cambridge.

Elder, J. W. 1959 *J. Fluid Mech.* **5**, 355.

Jackson, N. A. 1972 *J. Roy. Aero. Soc.*, 251.

Kotansky, D. R. 1966 *A.I.A.A. J.* **4**, 1490.

Lau, T. L. & Baines, W. D. 1968 *J. Fluid Mech.* **33**, 721.

Livesey, J. L. & Laws, E. M. 1972 *A.I.A.A. Paper*, no. 72–165.

Livesey, J. L. & Laws, E. M. 1973 *J. Fluid Mech.* **59**, 737.

Livesey, J. L. & Turner, J. T. 1964 *J. Fluid Mech.* **20**, 201.

Maull, D. J. 1969 The wake characteristics of a bluff body in a shear flow. *Aerodynamics of Atmospheric Shear Flows. Proc. Agard. Conf.* no. 48.

Owen, P. R. & Zienkiewicz, K. H. 1957 *J. Fluid Mech.* **2**, 521.

Rose, W. G. 1970 *J. Fluid Mech.* **44**, 767.

Taylor, G. I. & Batchelor, G. K. 1949 *Quart. J. Mech. Appl. Math.* **2**, 1.

Turner, J. T. 1969 *J. Fluid Mech.* **36**, 367.